

γ induced multiparticle emissions of medium mass nuclei at intermediate energies

Tapan Mukhopadhyay¹ and D. N. Basu²

Variable Energy Cyclotron Centre, 1/AF Bidhan Nagar, Kolkata 700 064, India *

(Dated: October 30, 2019)

A comprehensive analysis of multiparticle emissions following photon induced reactions at intermediate energies is provided. Photon induced reaction is described in the energy range of $\sim 30 - 140$ MeV with an approach based on the quasideuteron nuclear photoabsorption model followed by the process of competition between light particle evaporation and fission for the excited nucleus. The evaporation-fission process of the compound nucleus is simulated in a Monte-Carlo framework. The study shows almost no fission events for the medium mass nuclei and reproduces satisfactorily well the available experimental data of photonuclear reaction cross sections at energies $\sim 30 - 140$ MeV.

Keywords: Photonuclear reactions; Photofission; Nuclear fissility; Monte-Carlo

PACS numbers: 25.20.-x, 25.20.Dc, 25.85.Jg, 24.10.Lx

With energetic incident photon it is possible to induce nuclear reactions including fission in most elements. Photonuclear reactions in different energy ranges like giant dipole resonance (GDR) and quasideuteron (QD) energy regions have been studied in the past as they provide a wide range of information either on the initial nuclear excitation mechanism or on characteristics of the compound nucleus decay channels. In fact photoneutron cross sections in the GDR energy region have been compiled [1] for most of the nuclei in the periodic table, while measurements in the QD region were mainly focussed on heavy nuclei, thus leading to a lack of study on intermediate nuclei. For heavier nuclei, particularly for actinides and preactinides, with high enough energy of incident photons, the dominant reaction mechanism is fission where photofission cross sections are quite large [2]. With decreasing mass of the target nucleus and energy of incident photon, fission probability decreases whereas other reaction channels such as (γ, xn) and $(\gamma, xnypp)$ type become more important. Thus it becomes important to study the photonuclear reactions in the intermediate energy range for medium mass elements. Such investigations of multiparticle emissions following photon induced reactions in the intermediate energy region in medium mass elements may reveal important features of the nature of the photoabsorption mechanism as well as the decay channel characteristics.

The aim of the present work is to investigate photonuclear reactions of (γ, xn) and $(\gamma, xnypp)$ type. Present study is restricted to the QD region which is above the GDR or the isovector giant quadrupole resonance (IVGQR) regions and below the pion threshold. The different photonuclear reactions for V, Zn, Sn, Ce, Sm, Yb, Ta, Au, Pb and Bi are consistently described as a two step process. In the rapid stage of a photonuclear reaction, the incoming γ is assumed to be absorbed by a neutron-proton [n-p] pair inside the nucleus. The rapid

stage is then followed by a subsequent de-excitation of the compound nucleus (CN) via evaporation. Such a statistical decay of the CN is the slow stage of a photonuclear reaction. The quantitative description of the process is based on the liquid drop model (LDM) for nuclear fission by Bohr and Wheeler [3] and the statistical model of nuclear evaporation developed by Weisskopf [4]. For this slow stage, an evaporation Monte-Carlo routine, based on the Weisskopf statistical theory, to address the de-excitation of the CN in terms of the competition between particle evaporation and nuclear fission, is used.

The dominant mechanism for nuclear photoabsorption at intermediate energies is described by the QD model [5] which is employed to access [6] the total photoabsorption cross section in nuclei. It is based on the assumption that the incident photon is absorbed by a correlated n-p pair inside the nucleus, leaving the remaining nucleons as spectators. Such an assumption is enforced when wavelength of the incident photon is small compared to nuclear dimensions. The total nuclear photoabsorption cross section σ_a^T is then proportional to the available number of n-p pairs inside the nucleus and also to the free deuteron photodisintegration cross section $\sigma_d(E_\gamma)$:

$$\sigma_a^T(E_\gamma) = \frac{L}{A} N Z \sigma_d(E_\gamma) e^{-D/E_\gamma} \quad (1)$$

where N , Z and A are the neutron, proton and mass numbers respectively, $\frac{L}{A}$ factor represents the fraction of correlated n-p pairs and the function e^{-D/E_γ} accounts for the reduction of the n-p phase space due to the Pauli exclusion principle. A systematic study of total nuclear photoabsorption cross section data in the intermediate energy range shows that $D = 0.72A^{0.81}$ MeV [7]. The free deuteron photodisintegration cross section [8] is given by

$$\sigma_d(E_\gamma) = \frac{61.2 [E_\gamma - B]^{3/2}}{E_\gamma^3} \text{ [mb]} \quad (2)$$

where $B = 2.224$ MeV is the binding energy of the deuteron. The QD model [5, 6] of nuclear photoabsorp-

*E-mail 1: tkm@veccal.ernet.in; E-mail 2: dnb@veccal.ernet.in

tion is used together with modern rms radius data to obtain Levinger's constant $L = 6.8 - 11.2A^{-2/3} + 5.7A^{-4/3}$ of nuclei throughout the Periodic Table and is in good agreement [9] with those obtained from the experimentally measured σ_a^T values.

At the QD energy range, as a consequence of the primary photointeraction, $\gamma + (n+p) \rightarrow n^* + p^*$, in most of the cases excited compound nuclei are formed with the same composition as target nucleus where both neutron and proton are retained inside the nucleus and the probabilities that either neutron escapes or proton escapes or both neutron and proton escape from the nucleus are extremely low. Hence the recoiling nucleus can be viewed as a compound nucleus having the same composition as the target nucleus but with excitation energy $E^* = m_0c^2[(1 + 2E_\gamma/m_0c^2)^{1/2} - 1]$ [10] where E_γ is the incident photon energy and m_0 is the rest mass of the nucleus before photon absorption. This excited compound nucleus then undergoes successive evaporation of neutrons, protons and light particles and fission. Hence the photonuclear reaction cross section σ_r is a product of the nuclear photoabsorption cross section σ_a^T and the statistical decay probability p for a reaction channel and is, therefore, given by $\sigma_r(E_\gamma) = \sigma_a^T(E_\gamma)p$. The decay probability p is basically the branching ratio Γ_r/Γ where Γ_r and Γ are the partial and total reaction widths respectively.

The evaporation stage is calculated applying the statistical theory [4]. The decay of the CN takes into account all accessible channels, with the related branchings calculated in terms of the nuclear level densities of the daughter nuclei. The basic steps are the calculations of the relative probabilities between the competing channels (particle evaporation and nuclear fission). The probability of fission relative to neutron emission is calculated using Vandenbosch-Huizenga's equation [11] given by

$$\frac{\Gamma_f}{\Gamma_n} = \frac{K_0 a_n [2(a_f E_f^*)^{1/2} - 1]}{4A^{2/3} a_f E_n^*} \exp [2[(a_f E_f^*)^{1/2} - (a_n E_n^*)^{1/2}]] \quad (3)$$

where $E_n^* = E^* - B_n$ and $E_f^* = E^* - B_f$ are the nuclear excitation energies after the emission of a neutron and after fission, respectively, where B_n is the binding energy of the emitted neutron. Γ_n and Γ_f are the partial widths for the decay of the excited compound nucleus via neutron emission and fission, respectively, and the parameters a_n and a_f are the level density parameters for the neutron emission and the fission, respectively and $K_0 = \hbar^2/2mr_0^2$ where m and r_0 are the neutron mass and radius parameter respectively. The emission probability of particle k relative to neutron emission is calculated according to the Weisskopf's statistical model [4]

$$\frac{\Gamma_k}{\Gamma_n} = \left(\frac{\gamma_k}{\gamma_n}\right) \left(\frac{E_k^*}{E_n^*}\right) \left(\frac{a_k}{a_n}\right) \exp [2[(a_k E_k^*)^{1/2} - (a_n E_n^*)^{1/2}]] \quad (4)$$

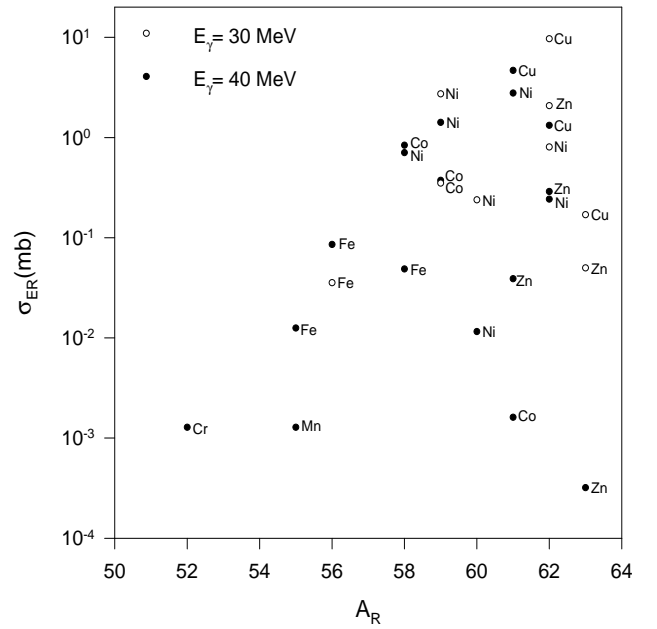


FIG. 1: The plots of cross sections σ_{ER} as a function of mass number A_R of the evaporation residues resulting from (γ, xn) and $(\gamma, xnyp)$ types of reactions for ^{64}Zn at $E_\gamma = 30, 40$ MeV.

where a_k is the level density parameter for the emission of the particle k , $\gamma_k/\gamma_n = 1$ for $k = p$, 2 for $k = {}^4\text{He}$, 1 for $k = {}^2\text{H}$, 3 for $k = {}^3\text{H}$ and 2 for $k = {}^3\text{He}$. $E_k^* = E^* - (B_k + V_k)$ is the nuclear excitation energy after the emission of particle k [12]. B_k are the binding energies of the emitted particles and V_k are the Coulomb potentials. The evaporation-fission competition of the compound nucleus is then described in the framework of a projection angular momentum coupled [13] Monte-Carlo routine [14]. Any particular reaction channel r is then defined as the formation of the compound nucleus via photoabsorption and its decay via particle emission or fission. Thus, fission is considered as a decay mode. The photonuclear reaction cross sections σ_r are calculated using the equation $\sigma_r = \sigma_a^T n_r/N$ where n_r is the number of events in a particular reaction channel r and N is total number of events that is the number of the incident photons.

Each calculation is performed with 40000 events using a Monte-Carlo technique for the evaporation-fission calculation. This provides a reasonably good computational statistics. Cross section $\sigma_r(E_\gamma)$ for any particular reaction channel r is then calculated using the equation $\sigma_r(E_\gamma) = \sigma_a^T(E_\gamma)n_r/N$. Detailed calculations have been performed for ^{51}V , ^{64}Zn , ^{118}Sn , ^{140}Ce , ^{154}Sm , ^{174}Yb , ^{181}Ta , ^{197}Au , ^{208}Pb and ^{209}Bi at $E_\gamma = 30$ MeV to 140 MeV and in Table I the results for (γ, xn) and $(\gamma, xnyp)$ reaction cross sections are provided. The statistical error in the theoretical calculations for the photonuclear reaction cross sections can be estimated using the equation $\sigma_r \pm \Delta\sigma_r = \sigma_a^T [n_r \pm \sqrt{n_r}]/N$ which implies that $\Delta\sigma_r = \sqrt{\sigma_a^T \sigma_r/N}$. In Fig.1 the plots of cross sec-

TABLE I: Photofission cross section and three largest photonuclear reaction cross sections in $(\gamma, xnypp)$ decay channels. The number of evaporated neutrons x and protons y are provided as (x, y) adjacent to each reaction cross sections.

Target nuclei	Z^2/A	Calculated quantity [mb]	E_γ [MeV] 30	E_γ [MeV] 40	E_γ [MeV] 60	E_γ [MeV] 80	E_γ [MeV] 100	E_γ [MeV] 120	E_γ [MeV] 140
^{51}V	10.37	σ_a^T	14.11	10.92	7.07	5.01	3.78	2.97	2.42
		$\sigma_r(\gamma, xnypp)$	10.76 (2,0)	4.30 (3,0)	3.46 (3,1)	1.80 (4,1)	0.95 (4,2)	0.55 (5,2)	0.31 (5,3)
			2.72 (1,1)	2.36 (2,0)	1.12 (4,0)	0.87 (3,2)	0.58 (5,2)	0.38 (5,3)	0.25 (7,4)
			0.32 (1,0)	2.28 (2,1)	0.52 (2,2)	0.46 (4,2)	0.49 (5,1)	0.26 (4,3)	0.23 (8,4)
		σ_f	0.0	0.0	0.18×10^{-3}	0.25×10^{-3}	0.85×10^{-3}	1.71×10^{-3}	2.48×10^{-3}
^{64}Zn	14.06	σ_a^T	16.13	12.84	8.57	6.16	4.68	3.71	3.03
		$\sigma_r(\gamma, xnypp)$	9.67 (1,1)	4.67 (2,1)	3.19 (2,2)	1.64 (3,2)	0.82 (4,3)	0.54 (6,5)	0.43 (5,4)
			2.73 (3,2)	2.78 (1,2)	1.83 (4,3)	1.00 (5,3)	0.79 (5,4)	0.52 (5,3)	0.39 (6,5)
			2.08 (2,0)	1.42 (3,2)	1.03 (3,1)	0.67 (4,4)	0.50 (4,2)	0.40 (6,4)	0.32 (6,6)
		σ_f	0.0	0.0	0.0	0.15×10^{-3}	0.0	0.28×10^{-3}	0.45×10^{-3}
^{118}Sn	21.19	σ_a^T	19.32	17.21	12.84	9.76	7.67	6.22	5.16
		$\sigma_r(\gamma, xnypp)$	12.95 (2,0)	15.03 (3,0)	9.44 (5,0)	5.74 (6,0)	2.93 (8,0)	1.63 (9,0)	1.28 (9,1)
			6.33 (3,0)	1.91 (4,0)	2.57 (4,0)	2.12 (7,0)	2.03 (7,0)	1.57 (8,1)	0.97 (10,0)
			0.04 (1,1)	0.14 (2,1)	0.34 (4,1)	0.86 (5,1)	1.06 (7,1)	0.69 (8,0)	0.69 (10,0)
		σ_f	0.0	0.0	0.0	0.0	0.0	0.0	0.0
^{140}Ce	24.03	σ_a^T	19.37	18.00	14.01	10.88	8.66	7.08	5.91
		$\sigma_r(\gamma, xnypp)$	16.06 (2,0)	15.96 (3,0)	11.35 (5,0)	4.81 (6,0)	4.19 (8,0)	2.14 (9,0)	1.44 (10,1)
			3.23 (3,0)	1.66 (4,0)	1.48 (4,0)	3.94 (7,0)	1.45 (7,1)	1.43 (8,1)	1.03 (9,1)
			0.06 (1,1)	0.25 (2,1)	0.58 (4,1)	1.04 (5,1)	1.15 (7,0)	0.94 (10,0)	0.72 (10,0)
		σ_f	0.0	0.0	0.0	0.0	0.0	0.0	0.0
^{154}Sm	24.96	σ_a^T	19.07	18.20	14.54	11.44	9.19	7.55	6.32
		$\sigma_r(\gamma, xnypp)$	17.82 (3,0)	17.05 (4,0)	11.44 (6,0)	7.62 (8,0)	4.66 (10,0)	3.54 (11,0)	2.50 (12,0)
			0.84 (3,0)	1.61 (7,0)	2.04 (7,0)	3.05 (9,0)	1.45 (10,0)	0.84 (13,0)	
			0.42 (4,0)	0.28 (5,0)	1.28 (5,0)	1.12 (9,0)	0.42 (10,2)	0.76 (12,0)	0.64 (11,1)
		σ_f	0.0	0.0	0.0	0.0	0.0	0.0	0.0
^{174}Yb	28.16	σ_a^T	18.67	18.49	15.33	12.29	9.97	8.25	6.95
		$\sigma_r(\gamma, xnypp)$	18.02 (3,0)	17.38 (4,0)	11.72 (6,0)	5.79 (8,0)	5.65 (9,0)	3.27 (11,0)	2.92 (12,0)
			0.62 (2,0)	1.04 (3,0)	3.34 (5,0)	5.64 (7,0)	1.65 (8,0)	2.95 (10,0)	0.98 (11,0)
			0.03 (4,0)	0.05 (5,0)	0.08 (4,1)	0.30 (6,0)	1.64 (10,0)	0.44 (9,1)	0.91(13,0)
		σ_f	0.0	0.0	0.0	0.0	0.0	0.62×10^{-3}	0.0
^{181}Ta	29.44	σ_a^T	18.50	18.55	15.58	12.57	10.24	8.49	7.17
		$\sigma_r(\gamma, xnypp)$	17.57 (3,0)	17.18 (4,0)	11.68 (6,0)	5.92 (7,0)	6.16 (9,0)	3.24 (11,0)	2.80 (12,0)
			0.92 (2,0)	1.32 (3,0)	3.56 (5,0)	5.68 (8,0)	1.39 (10,0)	2.77 (10,0)	0.91 (11,1)
			0.01 (1,1)	0.01 (4,2)	0.08 (4,1)	0.29 (6,1)	1.34 (8,0)	0.59 (9,1)	0.89 (11,0)
		σ_f	0.0	0.0	0.0	3.1×10^{-3}	1.02×10^{-3}	1.7×10^{-3}	3.1×10^{-3}
^{197}Au	31.68	σ_a^T	17.97	18.55	16.03	13.12	10.78	8.99	7.62
		$\sigma_r(\gamma, xnypp)$	15.70 (3,0)	14.04 (4,0)	10.10 (6,0)	7.28 (7,0)	6.44 (9,0)	3.89 (10,0)	3.87 (12,0)
			2.28 (2,0)	4.49 (3,0)	5.77 (5,0)	4.91 (8,0)	2.28 (8,0)	3.27 (11,0)	0.86 (11,0)
			0.9×10^{-3} (1,1)	0.01 (2,1)	0.06 (4,1)	0.57 (6,0)	1.25 (10,0)	0.40 (10,1)	0.80 (13,0)
		σ_f	0.0	1.85×10^{-3}	9.22×10^{-3}	0.02	0.05	0.07	0.16
^{208}Pb	32.33	σ_a^T	17.48	18.39	16.21	13.39	11.07	9.27	7.88
		$\sigma_r(\gamma, xnypp)$	15.47 (3,0)	16.12 (4,0)	11.79 (6,0)	6.49 (8,0)	6.97 (9,0)	5.12 (11,0)	3.53 (12,0)
			2.01 (2,0)	2.23 (3,0)	4.27 (5,0)	6.46 (7,0)	2.41 (10,0)	2.61 (10,0)	2.16 (13,0)
			5.68×10^{-3} (4,0)	0.01 (5,0)	0.03 (4,1)	0.19 (6,0)	1.18 (8,0)	0.53 (12,0)	0.77 (11,0)
		σ_f	1.75×10^{-3}	0.02	0.06	0.12	0.20	0.33	0.44
^{209}Bi	32.96	σ_a^T	17.49	18.43	16.28	13.46	11.13	9.33	7.93
		$\sigma_r(\gamma, xnypp)$	15.71 (3,0)	15.91 (4,0)	10.90 (6,0)	6.65 (7,0)	6.60 (9,0)	3.97 (11,0)	2.40 (12,0)
			1.75 (2,0)	2.42 (3,0)	4.86 (5,0)	5.57 (8,0)	1.72 (10,0)	2.57 (10,0)	1.36 (13,0)
			6.12×10^{-3} (2,1)	0.03 (2,1)	0.14 (4,1)	0.33 (6,1)	1.11 (8,0)	0.57 (10,1)	0.93 (11,1)
		σ_f	0.02	0.06	0.21	0.40	0.60	0.88	1.18

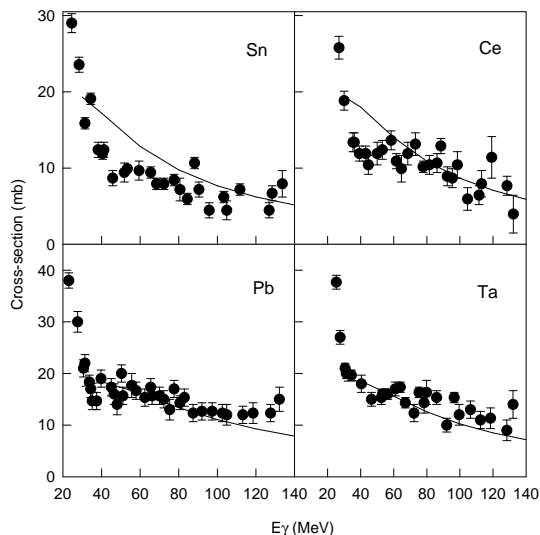


FIG. 2: Plots of total photoabsorption cross section versus photon energy. The continuous lines represent the total photoabsorption cross sections from the present calculation for ^{118}Sn , ^{140}Ce , ^{181}Ta and ^{208}Pb isotopes whereas the data points are those corresponding to the measured values [15] for natural targets of Sn, Ce, Ta and Pb.

tions of evaporation residues resulting from (γ, n) and (γ, np) type of reactions for ^{64}Zn for $E_\gamma = 30$ MeV and 40 MeV are shown as typical cases. In Fig.2 the plots of total photoabsorption cross section versus photon energy E_γ are presented. The continuous lines represent the total photoabsorption cross sections for Sn, Ce, Ta and Pb from the present calculations whereas the points with error bars are the experimental data [15]. Fig.3 shows the plots of average neutron multiplicities $\langle \nu \rangle = \sum_x x \sigma(\gamma, xnyp) / \sigma_a^T$ versus photon energy E_γ . The continuous lines represent the average neutron multiplicities for Sn, Ce, Ta and Pb from the present calculations whereas the points with error bars are the experimental data [16]. Considering the fact that the present calculations for photoabsorption cross sections are for isotopes ^{118}Sn , ^{140}Ce , ^{181}Ta and ^{208}Pb whereas the measurements [15] were performed using natural targets of Sn, Ce, Ta and Pb, present results agree quite closely with the available experimental data at intermediate energies. This effect is more pronounced in the plots for $\langle \nu \rangle$ where at E_γ above 50 MeV, present calculations gradually overestimate. This behaviour is expected

as neutron yields would be less in presence of lower mass isotopes in natural targets. It is worthwhile to mention here that the present formalism provides excellent estimates [2] for photofission cross sections of actinide and pre-actinide nuclei at intermediate energies.

In summary, the cross sections for the fission and the evaporation residues are calculated for photon induced nuclear reactions at intermediate energies. Monte-

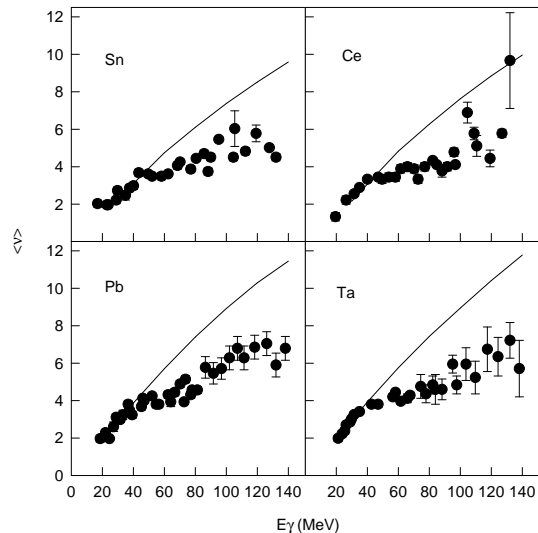


FIG. 3: Plots of average neutron multiplicities versus photon energy. The continuous lines represent the average neutron multiplicities from the present calculation for ^{118}Sn , ^{140}Ce , ^{181}Ta and ^{208}Pb isotopes whereas the data points are those corresponding to the measured values [16] for natural targets of Sn, Ce, Ta and Pb.

Carlo calculations for the evaporation-fission competition are performed assuming 40000 incident photons for each calculation which provides a reasonably good statistics for computationally stable results. Present calculations provide good estimates of cross sections for the reaction channels (γ, xn) and $(\gamma, xnyp)$ for nuclei ^{51}V , ^{64}Zn , ^{118}Sn , ^{140}Ce , ^{154}Sm , ^{174}Yb , ^{181}Ta , ^{197}Au , ^{208}Pb and ^{209}Bi at $E_\gamma = 30$ MeV to 140 MeV. No fission event has been observed below 40 MeV for these nuclei except few events in cases of ^{209}Bi and ^{208}Pb .

- [1] S. S. Dietrich and B. L. Berman, At. Data Nucl. Data Tables **38**, 199 (1988).
 [2] Tapan Mukhopadhyay and D. N. Basu, Phys. Rev. **C76**, 064610 (2007).
 [3] N. Bohr and J. A. Wheeler, Phys. Rev. **56**, 426 (1939).

- [4] V. F. Weisskopf, Phys. Rev. **52**, 295 (1937).
 [5] J. S. Levinger, Phys. Rev. **84**, 43 (1951).
 [6] J. S. Levinger, Phys. Letts. **82B**, 181 (1979).
 [7] M. L. Terranova, D. A. de Lima and J. D. Pinheiro Filho, Europhys. Lett. **9**, 523 (1989).

- [8] J. R. Wu and C. C. Chang, Phys. Rev. **C16**, 1812 (1977).
- [9] O. A. P. Tavares and M. L. Terranova, J. Phys. **G18**, 521 (1992).
- [10] D. N. Basu and Tapan Mukhopadhyay, arXiv: 0712.1129 [nucl-th].
- [11] R. Vandenbosch and J. R. Huizenga, *Nuclear Fission*, First ed., Academic Press, New York, (1973).
- [12] K. J. LeCouteur, Proc. Phys. Soc., London, **A63**, 259 (1950).
- [13] W. Hauser and H. Feshbach, Phys. Rev. **87**, 366 (1952).
- [14] Projection ang.mom. coupled evaporation code PACE2.
- [15] A. Leprêtre, H. Beil, R. Bergère, P. Carlos, J. Fagot, A. De Miniac and A. Veyssiére, Nucl. Phys. **A367**, 237 (1981).
- [16] A. Leprêtre, H. Beil, R. Bergère, P. Carlos, J. Fagot, A. Veyssiére and I. Halpern, Nucl. Phys. **A390**, 221 (1982).